Linear WFA Notes

Max Varverakis

July 2023

1 E_z

$$RadialPart = \int_0^\infty R(r')g_0(r,r')r'dr' \tag{1}$$

$$g_0(r,r') = 4\pi\left[I_0(k_pr)K_0(k_pr')\Theta(r'-r) + I_0(k_pr')K_0(k_pr)\Theta(r-r')\right] \tag{2}$$

$$R(r') = \begin{matrix} 1 & r' < \sigma_r \\ 0 & r' > \sigma_r \end{matrix} \tag{3}$$

What do we mean? . . .
r is the point where we observe the field
r' is the point where the charge is located
$R(r')$ is the distribution of charges
If we observe the field at location $r > \sigma_r$, this means that we "see" all the beam charge as within our observation point.

$$\begin{aligned} RadialPart_{r>\sigma_r} &= \int_0^{\sigma_r} 4\pi I_0(k_pr')K_0(k_pr)r'dr' \\ &= 4\pi r' I_1(k_pr')K_0(k_pr)\Big|_0^{\sigma_r} \\ &= 4\pi\sigma_r I_1(k_p\sigma_r)K_0(k_pr) \end{aligned} \tag{4}$$

because $\Theta(r-r') = 1$ for all $r > \sigma_r > r'$. So the radial component of E_z comes out to:

$$\boxed{E_z(r_{>\sigma_r}) = 4\pi\sigma_r I_1(k_p\sigma_r)K_0(k_pr)} \tag{5}$$

For $r < \sigma_r$, we have a contribution from both parts of Eqn. 2:

$$\frac{4\pi}{k_p}\int_0^{\sigma_r}\left[I_0(k_pr)K_0(k_pr')\Theta(r'-r)+I_0(k_pr')K_0(k_pr)\Theta(r-r')\right]k_pr'dr' \quad (6)$$

1. $r' < r$ invokes the term attached to $\Theta(r - r')$:

$$\begin{aligned}\int_0^r I_0(k_pr')K_0(k_pr)k_pr'dr' &= k_pr'I_1(k_pr')K_0(k_pr)\Big|_0^r \\ &= k_prI_1(k_pr)K_0(k_pr)\end{aligned} \quad (7)$$

2. $r' > r$ invokes the term attached to $\Theta(r' - r)$:

$$\begin{aligned}\int_r^{\sigma_r} I_0(k_pr)K_0(k_pr')k_pr'dr' &= -k_pr'I_0(k_pr)K_1(k_pr')\Big|_r^{\sigma_r} \\ &= k_prI_0(k_pr)\left[K_1(k_pr)-\frac{\sigma_r}{r}K_1(k_p\sigma_r)\right]\end{aligned} \quad (8)$$

Integrals were carried out using the identities listed in Sec. 4.

Plugging both integrals back into Eqn. 6 gives

$$\boxed{E_z(r_{<\sigma_r}) = 4\pi r\left[I_1(k_pr)K_0(k_pr)+I_0(k_pr)\left(K_1(k_pr)-\frac{\sigma_r}{r}K_1(k_p\sigma_r)\right)\right]} \quad (9)$$

2 E_r

For the radial electric field, we have a Green's function

$$\begin{aligned}g_1(r,r') =& 4\pi\left[I_1(k_pr)K_1(k_pr')\Theta(r'-r)+I_1(k_pr')K_1(k_pr)\Theta(r-r')\right] \quad (10)\\ \implies E_r(r) =& \int_0^\infty r'\frac{\partial}{\partial r}R(r')g_1(r,r')dr' \\ =& -\int_0^\infty r'\delta(r-\sigma_r)g_1(r,r')dr' \\ =& -\int_0^\infty r'\delta(r-\sigma_r)\left[I_1(k_pr)K_1(k_pr')\Theta(r'-r)+I_1(k_pr')K_1(k_pr)\Theta(r-r')\right]dr' \\ =& -4\pi\sigma_r\left[I_1(k_pr)K_1(k_p\sigma_r)\Theta(\sigma_r-r)+I_1(k_p\sigma_r)K_1(k_pr)\Theta(r-\sigma_r)\right]\end{aligned} \quad (11)$$

Thus, we have the following solution for the radial electric field depending on r:

1. $r < \sigma_r$ invokes the term attached to $\Theta(\sigma_r - r)$:

$$\boxed{E_r(r_{<\sigma_r}) = -4\pi\sigma_rK_1(k_p\sigma_r)I_1(k_pr)} \quad (12)$$

2. $r > \sigma_r$ invokes the term attached to $\Theta(r - \sigma_r)$:

$$\boxed{E_r(r_{>\sigma_r}) = -4\pi\sigma_rI_1(k_p\sigma_r)K_1(k_pr)} \quad (13)$$

3 Comparison to HiPACE++

Note that the plasma density ρ in HiPACE++ should be normalized to $e \cdot n_1$ whereas the plasma density from analysis only requires normalization to n_1.

3.1 Gaussian Beam

For the plots below, the number of electrons in the beam is $N_b = 4 \times 10^7$.

3.1.1 No Witness Beam

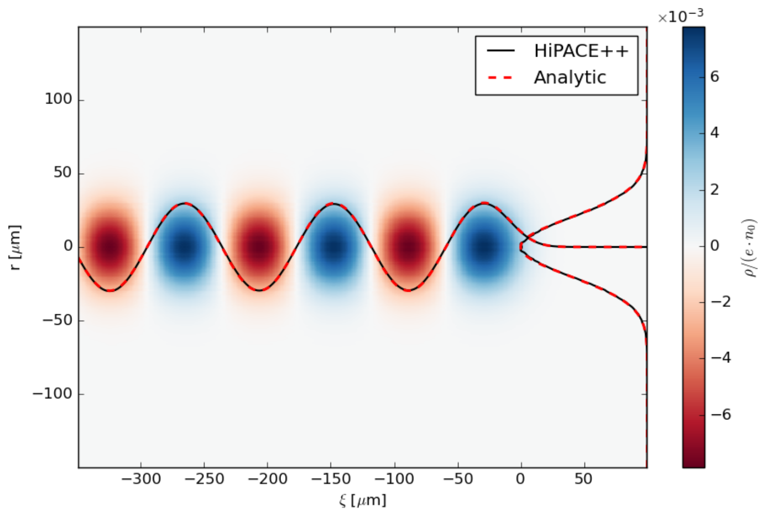

Figure 1: Plasma density from HiPACE++ simulation for a Gaussian beam. Analytical solution line-outs are overlaid in red.

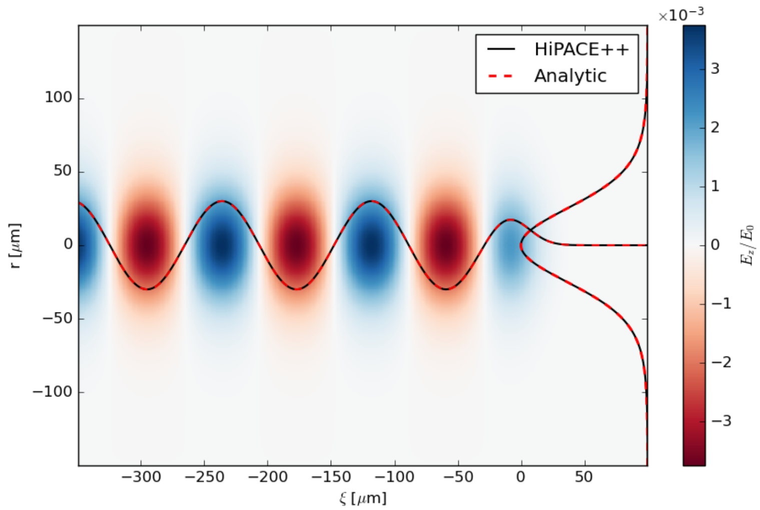

Figure 2: Normalized E_z from HiPACE++ simulation for a Gaussian beam. Analytical solution line-outs are overlaid in red.

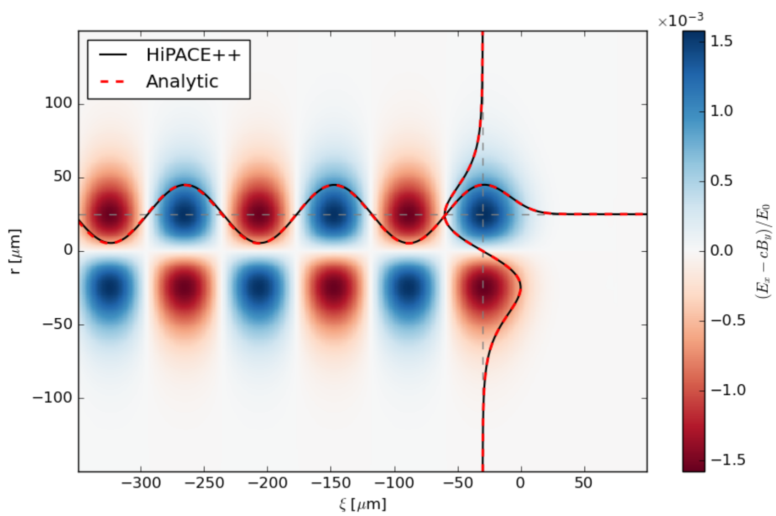

Figure 3: Normalized E_r from HiPACE++ simulation for a Gaussian beam. Analytical solution line-outs are overlaid in red. The longitudinal distribution is off-axis. Gray dashed lines indicate off-axis line out locations.

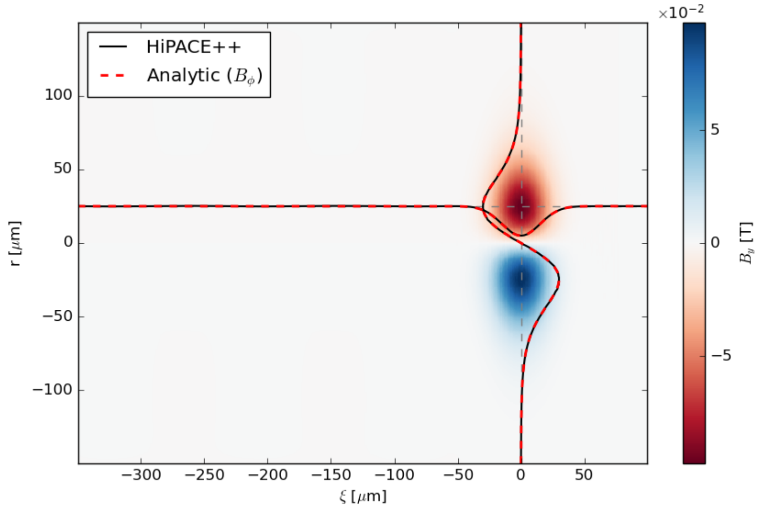

Figure 4: B_ϕ (B_y) from HiPACE++ simulation for a Gaussian beam. Analytical solution line-outs are overlaid in red. The longitudinal distribution is off-axis. Gray dashed lines indicate off-axis line out locations.

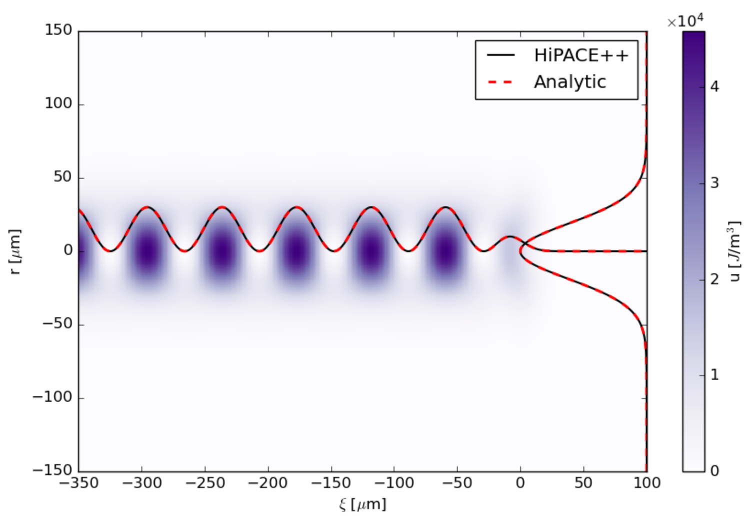

Figure 5: Energy density from HiPACE++ simulation for a Gaussian beam. Analytical solution line-outs are overlaid in red.

3.1.2 Witness Beam Loaded

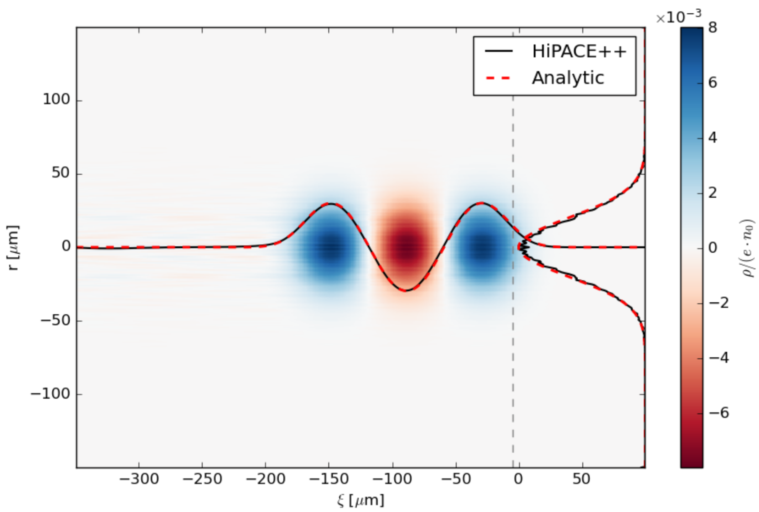

Figure 6: Plasma density from HiPACE++ simulation for two Gaussian beams. Analytical solution line-outs are overlaid in red.

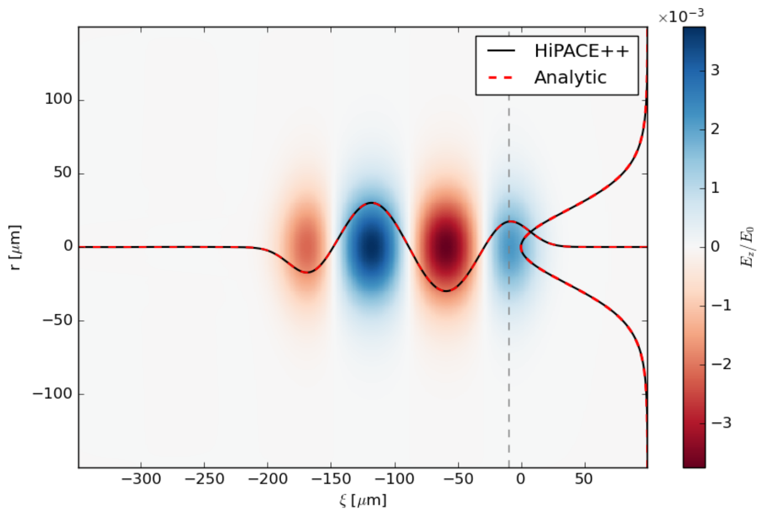

Figure 7: Normalized E_z from HiPACE++ simulation for two Gaussian beams. Analytical solution line-outs are overlaid in red.

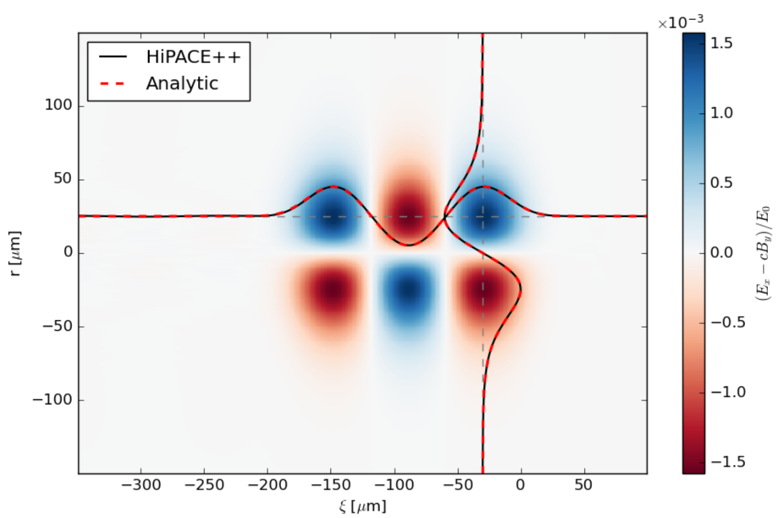

Figure 8: Normalized E_r from HiPACE++ simulation for two Gaussian beams. Analytical solution line-outs are overlaid in red. The longitudinal distribution is off-axis. Gray dashed lines indicate off-axis line out locations.

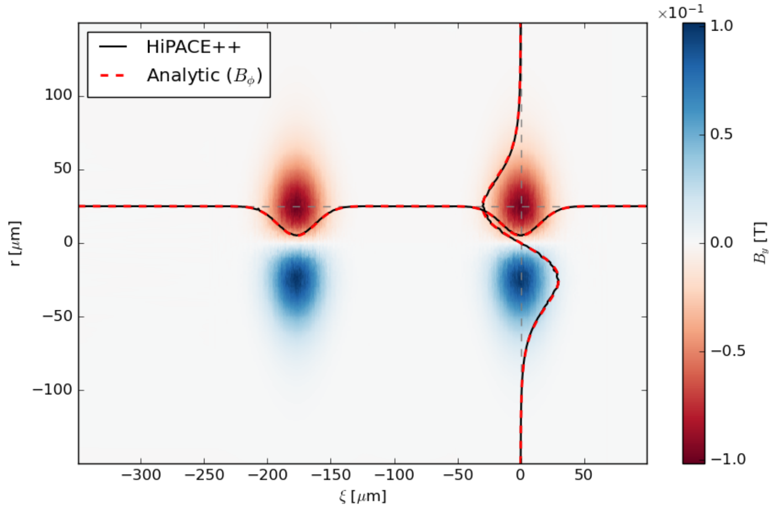

Figure 9: B_ϕ (B_y) from HiPACE++ simulation for two Gaussian beams. Analytical solution line-outs are overlaid in red. The longitudinal distribution is off-axis. Gray dashed lines indicate off-axis line out locations.

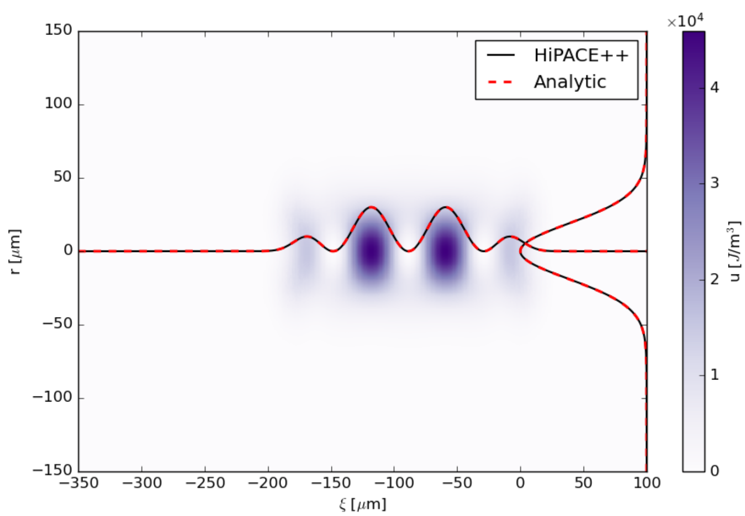

Figure 10: Energy density from HiPACE++ simulation for two Gaussian beams. Analytical solution line-outs are overlaid in red.

3.2 Heaviside Beam

For the plots below, the number of electrons in the beam is $N_b = 3.9972510 \times 10^7$.

3.2.1 No Witness Beam

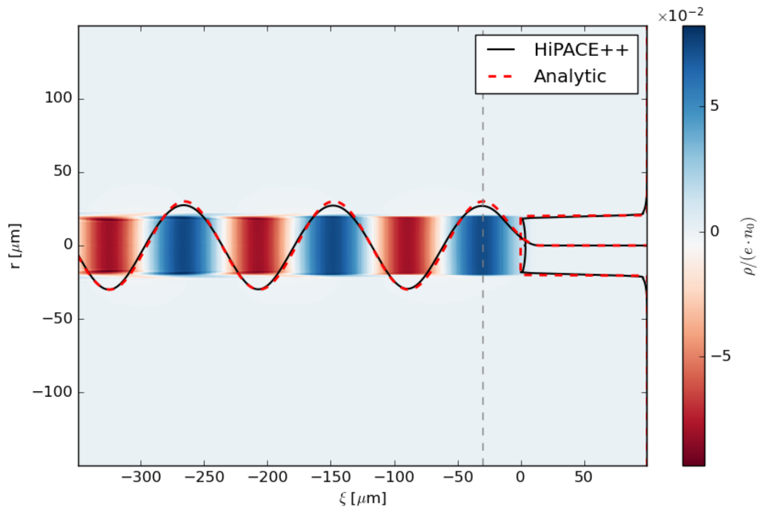

Figure 11: Plasma density from HiPACE++ simulation for a step-function beam. Analytical solution line-outs are overlaid in red. Gray dashed lines indicate off-axis line out locations.

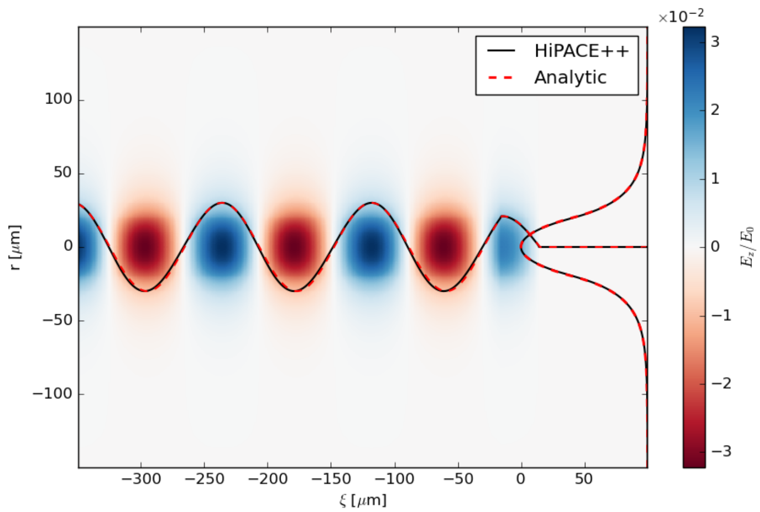

Figure 12: Normalized E_z from HiPACE++ simulation for a step-function beam. Analytical solution line-outs are overlaid in red.

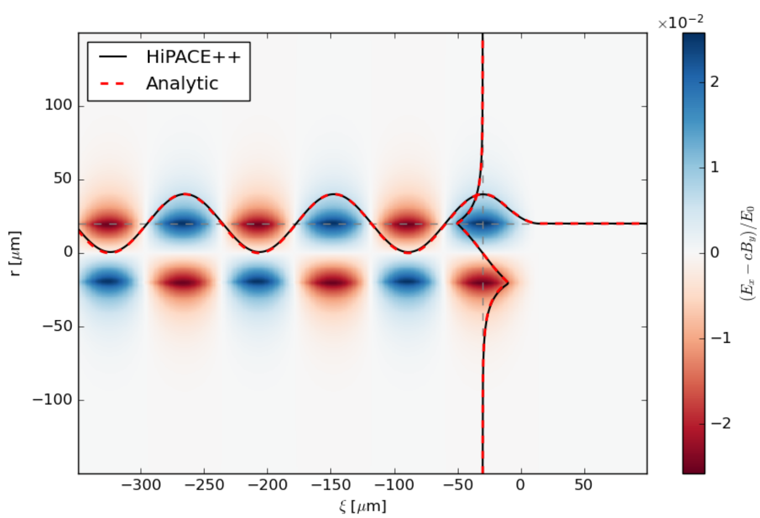

Figure 13: Normalized E_r from HiPACE++ simulation for a step-function beam. Analytical solution line-outs are overlaid in red. The longitudinal distribution is off-axis. Gray dashed lines indicate off-axis line out locations.

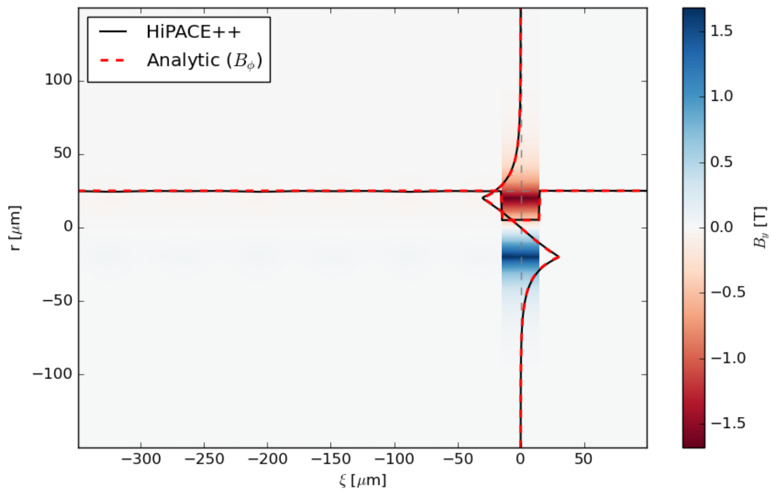

Figure 14: B_ϕ (B_y) from HiPACE++ simulation for a step-function beam. Analytical solution line-outs are overlaid in red. The longitudinal distribution is off-axis. Gray dashed lines indicate off-axis line out locations.

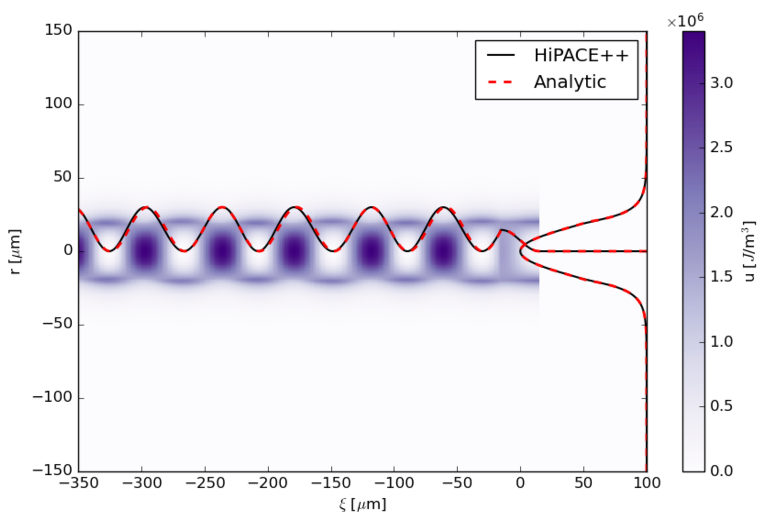

Figure 15: Energy density from HiPACE++ simulation for a step-function beam. Analytical solution line-outs are overlaid in red.

3.2.2 Witness Beam Loaded

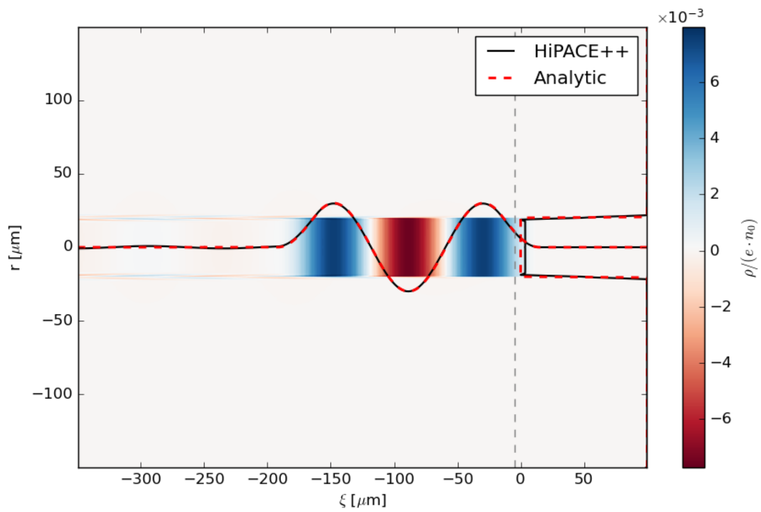

Figure 16: Plasma density from HiPACE++ simulation for two step-function beams. Analytical solution line-outs are overlaid in red. Gray dashed lines indicate off-axis line out locations.

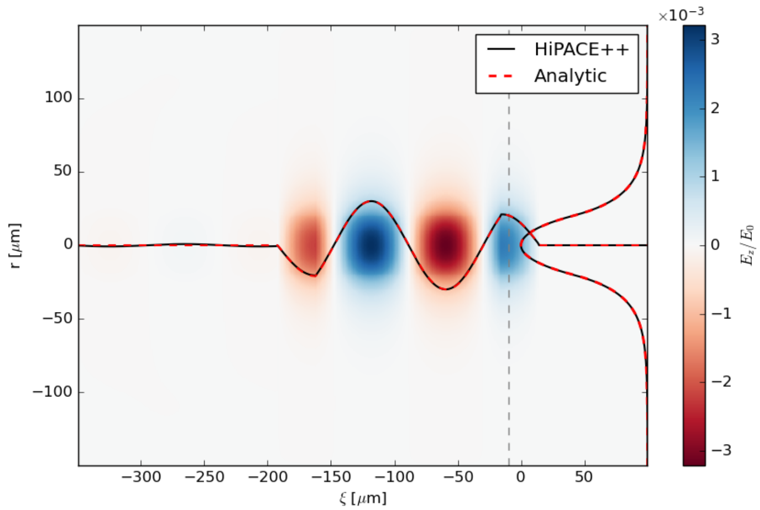

Figure 17: Normalized E_z from HiPACE++ simulation for two step-function beams. Analytical solution line-outs are overlaid in red.

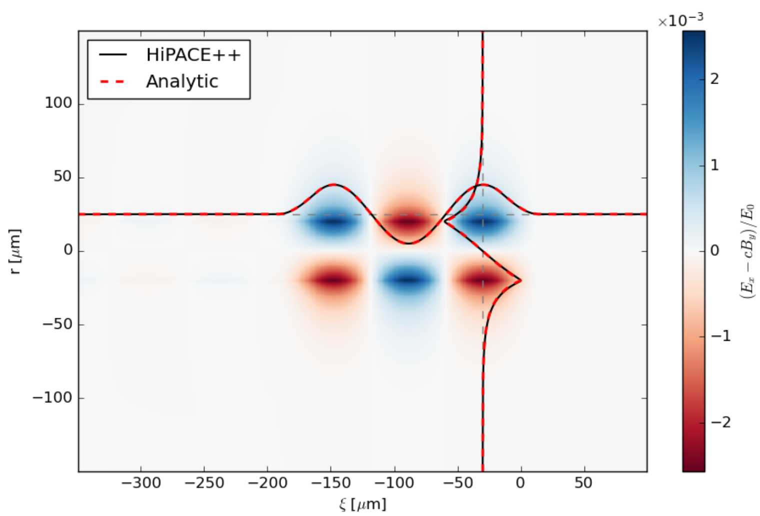

Figure 18: Normalized E_r from HiPACE++ simulation for two step-function beams. Analytical solution line-outs are overlaid in red. The longitudinal distribution is off-axis. Gray dashed lines indicate off-axis line out locations.

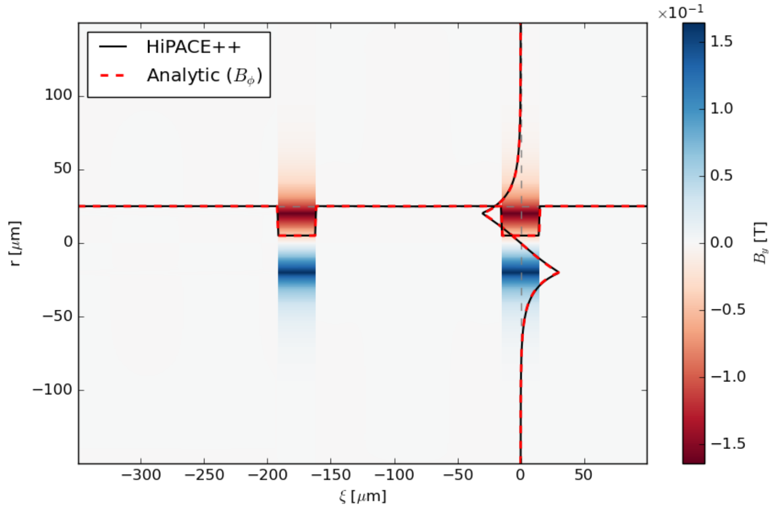

Figure 19: B_ϕ (B_y) from HiPACE++ simulation for two step-function beams. Analytical solution line-outs are overlaid in red. The longitudinal distribution is off-axis. Gray dashed lines indicate off-axis line out locations.

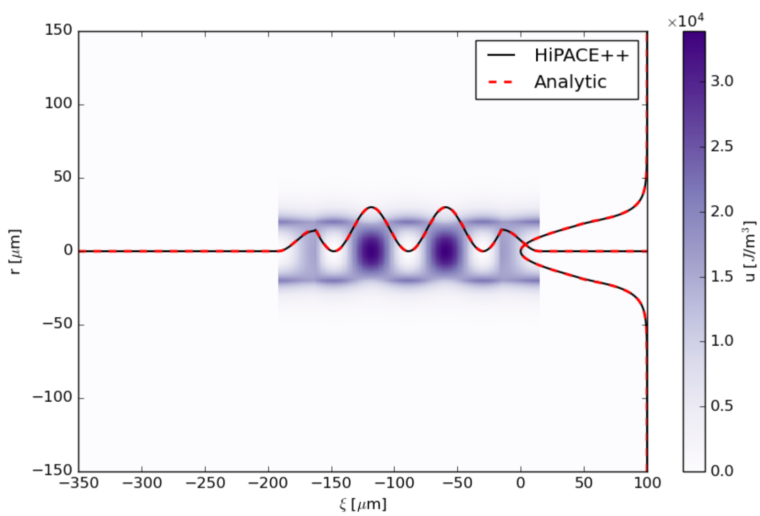

Figure 20: Energy density from HiPACE++ simulation for two step-function beams. Analytical solution line-outs are overlaid in red.

4 Modified Bessel Function Identities

$$\frac{d}{dx}\left[x^{\nu} I_{\nu}(x)\right] = x^{\nu} I_{\nu-1}(x) \tag{14}$$

$$\frac{d}{dx}\left[x^{\nu} K_{\nu}(x)\right] = -x^{\nu} K_{\nu-1}(x) \tag{15}$$